

# Preparation and Characterization of Novel Hybrid Materials Formed from (Ti,Sn)O<sub>2</sub> Nanoparticles and Polyaniline

Danielle C. Schnitzler,<sup>†</sup> Michelle S. Meruvia,<sup>‡</sup> Ivo A. Hümmelgen,<sup>‡</sup> and Aldo J. G. Zarbin<sup>\*,†</sup>

Departamento de Química, Universidade Federal do Paraná (UFPR), CP 19081, 81531-990, Curitiba, PR, Brazil, and Departamento de Física, Universidade Federal do Paraná (UFPR), CP 81531-990, Curitiba, PR, Brazil

Received April 23, 2003. Revised Manuscript Received August 11, 2003

This paper describes the synthesis and characterization of new organic/inorganic hybrid materials formed from the mixed oxide (Ti,Sn)O<sub>2</sub> nanoparticles and polyaniline (PANI). The preparation method is based on a sol–gel technique using titanium tetra-isopropoxide and tin tetrachloride as oxide precursors, and two synthetic routes to the hybrids formation were employed, based on the addition of aniline after or before the sol formation. Different amounts of aniline were used to verify this effect on the characteristics of the formed materials. Samples were characterized by thermal analysis, X-ray diffractometry, Raman, UV–vis, and FT-IR spectroscopy, transmission electron microscopy, cyclic voltammetry, and conductivity measurements. Results show that the different experimental routes are successful in producing hybrids formed by oxide nanoparticles or nanotubes and polyaniline in its conducting form, the emeraldine salt. There is little difference between the samples obtained by the two synthetic routes employed, except by the amount of polymer in the final material. The hybrids that contain approximately 10% weight of polyaniline are formed as a core/shell mixed oxide/polyaniline material.

## Introduction

Interest in the development of new inorganic/organic (nano)composites has grown in recent years due to a wide range of potential use of these materials.<sup>1–10</sup> These hybrids constitute a class of advanced composite materials with unusual properties, which can be used in many fields such as optics, ionics, electronics, and mechanics.

One important class of hybrid materials is that in which the organic fraction is composed of conducting polymers, such as polyaniline (PANI) or polypyrrole.<sup>11–19</sup>

In general, the formation of hybrids of conducting polymers and inorganic solids has the goal of obtaining composite materials with synergetic or complementary behaviors between the polymer and the inorganic matrixes. The properties of the designed composites will depend both on the characteristics of the polymers and on the nature of the inorganic matrixes. This approach can be very useful for obtaining materials with predetermined properties.

The unique properties of hybrid materials become more pronounced when at least one of the fractions occurs on the nanometric scale. Nanocomposites in which the polymer fraction occurs on the nanometric scale can be obtained by the encapsulation of conducting polymers within void spaces of inorganic host matrixes such as pores, cavities, tunnels, micelles, and interlayer domains.<sup>12,13,18,19</sup> We have recently prepared polypyrrole and polyaniline nanocomposites with several inorganic matrixes such as porous glasses,<sup>20–22</sup> layered materials,<sup>23,24</sup> and three-dimensional framework materials.<sup>25</sup>

Another interesting type of nanocomposites is that in which the inorganic material represents the nanometric phase. By this way, a great number of nanocomposites

\* Corresponding author. Tel: +55-41-3613297. Fax: +55-41-3613186. E-mail: aldo@quimica.ufpr.br.

<sup>†</sup> Departamento de Química.

<sup>‡</sup> Departamento de Física.

(1) Judeinstein, P.; Sanchez, C. *J. Mater. Chem.* **1996**, *6*, 511.

(2) Asefa, T.; Yoshina-Ishii, C.; MacLachlan, M. J.; Ozin, G. A. *J. Mater. Chem.* **2000**, *10*, 1751.

(3) Gomez-Romero, P.; Chojak, M.; Cuentas-Gallegos, K.; Asensio, J. A.; Kulesza, P. J.; Casan-Pastor, N.; Lira-Cantu, M. *Electrochem. Commun.* **2003**, *5*, 149.

(4) Boury, B.; Corriu, R. J. P. *Adv. Mater.* **2000**, *12*, 989.

(5) Kimizuka, N.; Kunitake, T. *Adv. Mater.* **1996**, *8*, 89.

(6) Giannelis, E. P. *Adv. Mater.* **1996**, *8*, 29.

(7) Kryszewski, M. *Synth. Met.* **2000**, *109*, 47.

(8) Backov, R.; Bonnet, B.; Jones, D. J.; Rozière, J. *Chem. Mater.* **1997**, *9*, 1812.

(9) Choudhury, K. R.; Winiarz, J. G.; Samoc, M.; Prasad, P. N. *Appl. Phys. Lett.* **2003**, *82*, 406.

(10) Valkenberg, M. H.; Holderich, W. F. *Catal. Rev.-Sci. Eng.* **2002**, *44*, 321.

(11) Kerr, T. A.; Wu, H.; Nazar, L. F. *Chem. Mater.* **1996**, *8*, 2005.

(12) Bein, T.; Enzel, P. *Angew. Chem., Int. Ed. Engl.* **1989**, *28*, 1692.

(13) Lira-Cantú, M.; Gómez-Romero, P. *Chem. Mater.* **1998**, *10*, 698.

(14) Jang, S. H.; Han, M. G.; Im, S. S. *Synth. Met.* **2000**, *110*, 17.

(15) Mehrotra, V.; Keddie, J. L.; Miller, J. M.; Giannelis, E. P. *J. Non-Cryst. Solids* **1991**, *136*, 97.

(16) Wei, Y.; Yeh, J.-M.; Jin, D.; Jia, X.; Wang, J.; Jang, G.-W.; Chen, C.; Gumbs, R. W. *Chem. Mater.* **1995**, *7*, 969.

(17) Hori, T.; Kuramoto, N.; Tagaya, H.; Karasu, M.; Kadokawa, J.; Chiba, K. *J. Mater. Res.* **1999**, *14*, 7.

(18) Ruiz-Hitzky, E.; Aranda, P. *An. Quim.-Int. Ed.* **1997**, *93*, 197.

(19) Maia, D. J.; De Paoli, M.-A.; Alves, O. L.; Zarbin, A. J. G.; Neves, S. *Quim. Nova* **2000**, *23*, 204.

between conducting polymers and nanoparticles of different oxides such as TiO<sub>2</sub>, Fe<sub>2</sub>O<sub>3</sub>, and SnO<sub>2</sub> have been described.<sup>26–33</sup> Among the different compounds largely used as inorganic fractions in hybrids with conducting polymers, titanium dioxide has received particular attention in recent years.<sup>29–40</sup> Several reports involving the synthesis and characterization of different polypyrrole or polyaniline/TiO<sub>2</sub> hybrids have been described, aiming to obtain materials that find applications in electrochromic devices, nonlinear optical systems, photoelectrochemical devices, and so forth.<sup>29,34–38</sup> For example, the combination of the n-type semiconductor property of nanoparticulated TiO<sub>2</sub> with the p-type of polyaniline has been considered as being responsible for an improvement in the polyaniline photocurrent values due to the occurrence of exciton dissociation at their interface.<sup>30</sup>

TiO<sub>2</sub>/conducting polymer hybrids have been prepared by the electrochemical polymerization of the monomer on a film of the oxide<sup>36,37</sup> or by chemical polymerization of the monomer in a dispersion which contains the oxide (nano)particles.<sup>26,30,33,34,40</sup> The experimental procedure is fundamental in controlling the properties of the resulting material. Variables such as size and shape of the oxide particles, degree of the dispersion, kind of interaction and interface between the organic and the inorganic phases, among others, have direct influence on properties such as conductivity, piezoresistivity, and photocurrent.

Recently, we developed a sol–gel route to a mixed titanium–tin oxide nanoparticle with anatase structure.<sup>41</sup> We believe that the utilization of this (Ti,Sn)O<sub>2</sub> in hybrids with conducting polymers can result in new

materials with useful properties, once this synergetic effect has been observed in hybrids with TiO<sub>2</sub>. In this paper we report the in situ synthesis and characterization of some hybrid materials between (Ti,Sn)O<sub>2</sub> nanoparticles and the conducting polymer polyaniline.

## Experimental Section

Titanium tin oxide was produced as reported,<sup>41</sup> but HCl was used rather than HNO<sub>3</sub>, which was used before: in a glovebox 0.5 mL of SnCl<sub>4</sub> (Riedel) was previously stirred with 12.5 mL of 2-propanol for 10 min, followed by the addition of 12.5 mL of titanium isopropoxide (TTIP). This mixture was stirred for 10 min more and subsequently was slowly added to 75 mL of Milli-Q H<sub>2</sub>O into which 0.2 mL of concentrated chloridric acid solution was added previously. Precipitation occurred immediately. The precipitate was then peptized with the available HCl at 60 °C for 8 h in a reflux system. After this the reaction was stirred for 8 h at room temperature, followed by evaporation of 2-propanol and water at 55 °C for a week. The 55 °C drying gel was stored in a desiccator for further characterization.

Two different routes were used to produce the oxide/PANI hybrids as follows:

(i) Group 1: aniline was added previously to hydrolysis. In a glovebox a suitable amount of fresh distilled aniline (0.242 or 0.675 mL) was added to the above-described solution formed from TIPP and SnCl<sub>4</sub>. The new mixture of aniline, TIPP, and SnCl<sub>4</sub> was stirred for 10 min more and subsequently added to react with water in a similar way as described above for the synthesis of (Ti,Sn)O<sub>2</sub>. The formed white precipitate was also peptized at 60 °C for 8 h following by stirring at room temperature for additional 8 h. After this, to polymerize the aniline, 30 mL of a (NH<sub>4</sub>)<sub>2</sub>S<sub>2</sub>O<sub>8</sub> aqueous solution containing 1.0 mol L<sup>-1</sup> of HCl was added to the reactional media, and the mixture was stirred at room temperature for 3 h. The (NH<sub>4</sub>)<sub>2</sub>S<sub>2</sub>O<sub>8</sub> solution was prepared to maintain the aniline/(NH<sub>4</sub>)<sub>2</sub>S<sub>2</sub>O<sub>8</sub> molar ratio constant, by the dissolution of 0.301 or 0.851 g of (NH<sub>4</sub>)<sub>2</sub>S<sub>2</sub>O<sub>8</sub> (to aniline amount of 0.242 or 0.675 mL, respectively) in 30 mL of a 1.0 mol L<sup>-1</sup> HCl aqueous solution. The resulting green solid was separated by centrifugation, washed five times with distilled water, dried at 40 °C for a week, and stored in desiccator for further characterization. The sample obtained with the minor initial amount of aniline (0.242 mL) will be referred to here as **TiSn/PANI-1A** and the sample obtained with the higher amount of aniline (0.675 mL) as **TiSn/PANI-1B**.

(ii) Group 2: aniline added after the hydrolysis and peptization. After all the synthetic steps to the synthesis of (Ti,Sn)O<sub>2</sub> described above, and before the evaporation of 2-propanol and water, a suitable amount of fresh distilled aniline (0.242 or 0.675 mL) was added to the media containing the (Ti,Sn)O<sub>2</sub> sol. After 10 min under stirring, 30 mL of the same (NH<sub>4</sub>)<sub>2</sub>S<sub>2</sub>O<sub>8</sub> solution described in item (i) was added to the system. The mixture was stirred at room temperature for 3 h, and the resulting green solid was separated, washed, dried, and stored as described above. The sample obtained with the minor initial amount of aniline (0.242 mL) will be referred to here as **TiSn/PANI-2A** and the sample obtained with the higher amount of aniline (0.675 mL) as **TiSn/PANI-2B**.

XRD patterns were obtained in a Phillips diffractometer, using Co K $\alpha$  radiation with 40 kV and 20 mA, at a 0.2° scan rate (in 2 $\theta$ ). The room-temperature measurements were performed with the samples spread on a conventional glass sample holder. Powder silicon reflections were used for 2 $\theta$  calibration. The areas of the XRD peaks were evaluated by Gaussian deconvolution using the Origin 5.0 program. The crystallite diameter was determined employing peak-broadening analysis utilizing Scherrer's equation.

The FT-IR spectra of the samples were obtained with a Bomem MB-100 spectrophotometer in the 4000–400-cm<sup>-1</sup> range with 32 scans. The samples were prepared into KBr pellets.

(20) Zarbin, A. J. G.; De-Paoli, M. A.; Alves, O. L. *Synth. Met.* **1999**, *99*, 227.

(21) Maia, D. J.; Zarbin, A. J. G.; Alves, O. L.; De-Paoli, M. A. *Adv. Mater.* **1995**, *7*, 792.

(22) Sotomayor, P. T.; Raimundo, I. M.; Zarbin, A. J. G.; Rohwedder, J. J. R.; Neto, G. O.; Alves, O. L. *Sens. Actuators, B* **2001**, *74*, 157.

(23) Gonçalves, A. B.; Mangrich, A. S.; Zarbin, A. J. G. *Synth. Met.* **2000**, *114*, 119.

(24) Zarbin, A. J. G.; Maia, D. J.; De-Paoli, M. A.; Alves, O. L. *Synth. Met.* **1999**, *102*, 1277.

(25) Beleze, F. A.; Zarbin, A. J. G. *Brazil. Chem. Soc.* **2001**, *12*, 542.

(26) Maeda, S.; Armes, S. P. *Chem. Mater.* **1995**, *7*, 171.

(27) Tang, B. Z.; Geng, Y. H.; Lam, J. W. Y.; Li, B. S.; Jing, X. B.; Wang, X. H.; Wang, F. S.; Pakhomov, A. B.; Zhang, X. X. *Chem. Mater.* **1999**, *11*, 1581.

(28) Suri, K.; Annapoorni, S.; Sarkar, A. K.; Tandon, R. P. *Sens. Actuators, B* **2002**, *81*, 277.

(29) Hao, Y.; Yang, M.; Yu, C.; Cai, S.; Liu, M.; Fan, L.; Li, Y. *Sol. Energy Mater. Sol. Cells* **1998**, *56*, 75.

(30) Feng, W.; Sun, E.; Fujii, A.; Wu, H.; Nihara, K.; Yoshino, K. *Bull. Chem. Soc. Jpn.* **2000**, *73*, 2627.

(31) Su, S.-J.; Kuramoto, N. *Synth. Met.* **2000**, *114*, 146.

(32) Gurunathan, K.; Trivedi, D. C. *Mater. Lett.* **2000**, *45*, 262.

(33) Xia, H.; Wang, Q. *Chem. Mater.* **2002**, *14*, 2158.

(34) Nogueira, A. F.; Micaroni, L.; Gazotti, W. A.; De Paoli, M. A. *Electrochem. Commun.* **1999**, *1*, 262.

(35) Murakoshi, K.; Kogure, R.; Wada, Y.; Yanagida, S. *Chem. Lett.* **1997**, 471.

(36) Murakoshi, K.; Kogure, R.; Wada, Y.; Yanagida, S. *Sol. Energy Mater. Sol. Cells* **1998**, *55*, 113.

(37) Wang G.; Chen H.; Zhang H.; Yuan, C.; Lu, Z.; Wang, G.; Yang, W. *Appl. Surf. Sci.* **1998**, *135*, 97.

(38) Kobayashi, N.; Teshima, K.; Hirohashi, R. *J. Mater. Chem.* **1998**, *8*, 497.

(39) Kuwabata, S.; Takahashi, N.; Hirao, S.; Yoneyama, H. *Chem. Mater.* **1993**, *5*, 437.

(40) Somani, P. R.; Marimuthu, R.; Mulik, U. P.; Sainkar, S. R.; Amalnerkar, D. P. *Synth. Met.* **1999**, *106*, 45.

(41) Oliveira, M. M.; Schnitzler, D. C.; Zarbin, A. J. G. *Chem. Mater.* **2003**, *15*, 1903.

The Raman spectra were obtained in a Renishaw Raman Image spectrophotometer, coupled to an optical microscope that focuses the incident radiation down to an approximately 1- $\mu\text{m}$  spot. A He-Ne laser (emitting at 632.8 nm) was used, with incidence potency of 2 mW over the 2000–100- $\text{cm}^{-1}$  region.

TGA/DSC measurements were carried out simultaneously in Netzsch STA 409 equipment, in static air. Approximately 15 mg of each sample were analyzed between 20 and 1000  $^{\circ}\text{C}$  at 8  $^{\circ}\text{C min}^{-1}$  using alumina crucibles.

The UV-Vis spectra were collected in reflectance mode in a Shimadzu UV-2401 spectrophotometer, in the 190–900-nm region with the samples in powder, using  $\text{BaSO}_4$  as reference.

To measure the cyclic voltammetry, samples were suspended in distilled water and sonicated for 15 min. This suspension was carefully transferred to the surface of conducting glass (ITO) electrodes. After water evaporation (at room temperature) a uniform and transparent film was formed inside the ITO surface, which was used as a working electrode. Measurements were performed using a EG&G Princeton potentiostat, model 273A, interfaced to a PC computer. A one-compartment cell with a Pt wire as a counter electrode, a Ag/AgCl reference electrode, and a 1 mol  $\text{L}^{-1}$  HCl/NaCl aqueous solution as an electrolyte were used. The scan speed was 50  $\text{mV s}^{-1}$  and the potential range was from –200 to 1000 mV.

Films of the samples were prepared in a similar way to the one described above on the surface of a glass plate, and the electrical conductivity of these films was measured by the four-probe technique (four parallel Au stripes deposited by evaporation in a vacuum using a resistive crucible) in air and room temperature using a Keithley 220 current source and a Keithley 196 multimeter. To avoid sample degradation induced by high current density during electrical measurements, the conductivity was measured by applying a current of 1  $\mu\text{A}$ , 5  $\mu\text{A}$  and then increased stepwise (steps of 5  $\mu\text{A}$ ) up to the maximum of 100  $\mu\text{A}$ . The conductivity at each step corresponds to the average value of 50 recorded values taken for 300 s. Sample thickness was determined after electrical measurements using a surface profiler.

TEM measurements were done in a JEOL 120 KV instrument. The samples for observation were suspended in water and allowed to settle for 15 min. Then a drop of the supernatant dispersion was placed onto a carbon film supported by a copper grid.

## Results and Discussion

We recently described the mixed titanium tin oxide obtained according to the sol-gel route presented here as nanoparticles of a solid solution, with the tin atoms substituting the titanium in the anatase structure.<sup>41</sup> For the synthesis of the four hybrids, we introduced modifications in the synthetic procedure for the  $(\text{Ti,Sn})\text{O}_2$  in two different approaches. In the first one, we mixed the monomer aniline with the molecular precursors to the mixed oxide, and the hydrolysis was realized in this mixture. In this case, the oxide formation occurs in an environment that already contains the monomer. Second, we obtained the  $(\text{Ti,Sn})\text{O}_2$  sol and then added the aniline to it. In both cases the polymerization was realized using an acidic solution of ammonium persulfate. All the polymerizations were conducted in the same way, to compare the characteristics of the different samples obtained. Also, for each synthetic approach, two amounts of aniline were added, aiming to obtain hybrids with different relations between the inorganic and organic fraction and to investigate the effect of the initial aniline amount in the final product.

The thermal behavior of the hybrid samples was investigated by thermogravimetry (TG) and differential scanning calorimetry (DSC), and the results are shown

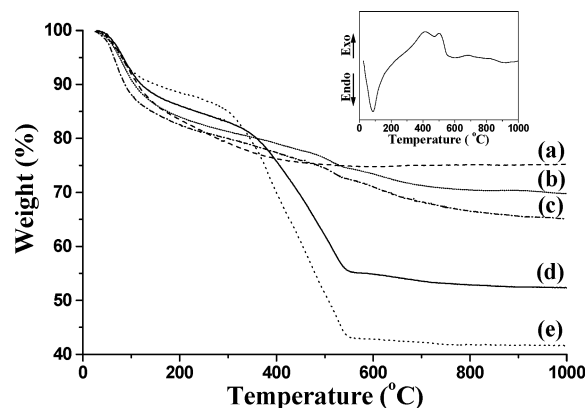


**Figure 1.** Thermogravimetric curves: (a)  $(\text{Ti,Sn})\text{O}_2$ ; (b) TiSn/PANI-2A; (c) TiSn/PANI-1A; (d) TiSn/PANI-1B; (e) TiSn/PANI-2B. The inset shows the DSC curve for the TiSn/PANI-1A sample.

in Figure 1. The 21.5% weight loss observed until 400  $^{\circ}\text{C}$  in the TG curve of pure  $(\text{Ti,Sn})\text{O}_2$  (Figure 1a) is attributed to the elimination of adsorbed water and alcohol and to the dehydroxylation process of surface-attached  $\text{H}_2\text{O}$  and OH groups, as reported before.<sup>41</sup> The hybrids TG curves also show weight losses between 30 and 300  $^{\circ}\text{C}$  attributed to the loss of water (from both the oxide and polymer surface) and acid dopant,<sup>42–44</sup> besides a well-differentiated behavior marked by a strong weight loss in the 300–550  $^{\circ}\text{C}$  range, attributed to degradation of the skeletal polyaniline chain structure.<sup>42–44</sup> This weight loss is correlated with two strong exothermic peaks in the DSC of the hybrid samples, at 412 and 504  $^{\circ}\text{C}$ , as can be seen in the inset of Figure 1. The DSC curve (which is representative for all the other hybrid samples) also show an endothermic peak centered at 88  $^{\circ}\text{C}$  (due to the water loss of the system) and an exothermic peak at 687  $^{\circ}\text{C}$  attributed to an anatase-rutile phase transition in the titanium tin mixed oxide.<sup>41</sup> The amount of polyaniline in each hybrid sample was estimated by CHN elemental analysis and is close to that stipulated by the weight loss in the 300–550  $^{\circ}\text{C}$  range on TG curves. The values found correspond to the following (in weight percent): 10.6, 27.5, 9.7, and 39.9 for the samples TiSn/PANI-1A, TiSn/PANI-1B, TiSn/PANI-2A, and TiSn/PANI-2B, respectively. As we can see, the fraction of polymer in both hybrid materials that were prepared with the minor initial amount of aniline (TiSn/PANI-1A and TiSn/PANI-2A) is very close, but in the samples TiSn/PANI-1B and TiSn/PANI-2B the amount of polymer obtained is very different, despite the volume of aniline initially used to form both these samples being the same.

The green color of all four samples obtained was the first evidence of the polyaniline formation in its conducting form, emeraldine salt (ES). The ES occurrence was confirmed by infrared (FT-IR), Raman, and reflectance UV-vis spectroscopy. The FT-IR spectra of the hybrid samples (not shown) present all the characteristic bands of ES, at 1604, 1570, 1478, 1307, 1238, 1134, 1048, 972, and 806  $\text{cm}^{-1}$ . Comparing between the

(42) Pielichowski, K. *Solid State Ionics* **1997**, *104*, 123.

(43) Matveeva, E. S.; Calleja, R. D.; Parkhutik, V. P. *Synth. Met.* **1995**, *72*, 105.

(44) Han, M. G.; Lee, Y. J.; Byun, S. W.; Im, S. S. *Synth. Met.* **2001**, *124*, 337.

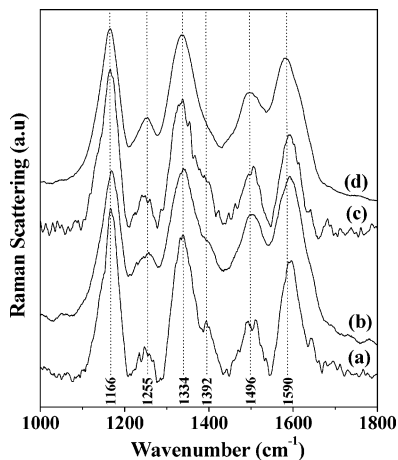


**Figure 2.** Resonance Raman spectra: (a) TiSn/PANI-1A; (b) TiSn/PANI-1B; (c) TiSn/PANI-2A; (d) TiSn/PANI-2B.

hybrids spectra, we can find some subtle differences, connected with the amount of PANI. Basically, the intensity of some ES bands (mainly, the polaron C–N stretching band at 1238 cm<sup>-1</sup> and the out-of-plane C–H bending band at 1048 cm<sup>-1</sup>) is affected by the amount of polyaniline in the hybrids. Similar results were observed in the TiO<sub>2</sub>/polyaniline hybrids reported by Somani et al.<sup>40</sup> and Feng et al.<sup>30</sup> and were explained due to the occurrence of interactions between the polymer and the oxide surface.

Figure 2 shows the resonance Raman spectra of hybrids and of the pure oxide. These spectra were collected with the 632.8-nm laser, the frequency of which is coincident with the visible absorption band assigned to the radical cation segment, as will be discussed later. By this way, as expected, the quinoid and semiquinoid Raman bands are very salient in the spectra. As we can see in Figure 2, all the hybrid spectra are very similar and are in agreement with the previously described spectra of pure emeraldine salt,<sup>45–49</sup> with the following main bands: ~1590 cm<sup>-1</sup> ( $\nu$  C=C of the quinoid rings), ~1496 cm<sup>-1</sup> ( $\nu$  C=N of the quinoid di-imina units), ~1334 cm<sup>-1</sup> ( $\nu$  C–N radical cation), ~1255 cm<sup>-1</sup> ( $\nu$  C–N benzene diamine units), and ~1166 cm<sup>-1</sup> (C–H bending of the quinoid rings). One interesting feature observed in Figure 2 is the occurrence of a band in 1392 cm<sup>-1</sup> in the Raman spectra of both the hybrid obtained with the minor amount of PANI (TiSn/PANI-1A and -2A, a and c, respectively, in Figure 2). This band does not occur in the TiSn/PANI-2B (maximum amount of PANI, Figure 2d) and appears as a shoulder in the spectrum of the TiSn/PANI-1B (Figure 2b), which is the sample that contains an intermediate amount of PANI. This band was already observed by Engert et al.<sup>50</sup> as one of the most intense bands in the resonance Raman spectrum of emeraldine salt excited

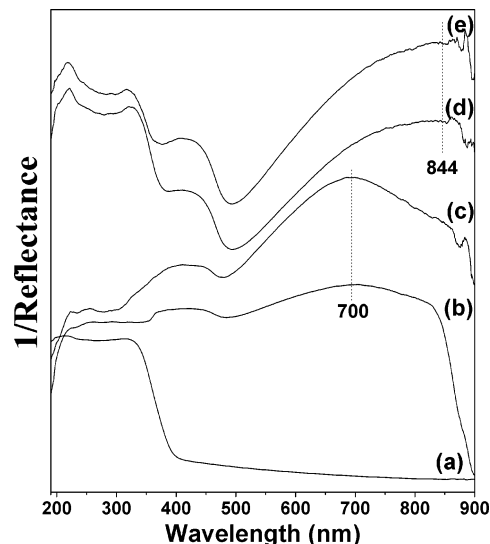


**Figure 3.** Reflectance UV-vis spectra: (a) (Ti,Sn)O<sub>2</sub>; (b) TiSn/PANI-2B; (c) TiSn/PANI-1B; (d) TiSn/PANI-2A; (e) TiSn/PANI-1A.

with the 1047-nm frequency laser (that is in resonance with the electronic absorption of free charge carriers in the metallic form of PANI) and can be associated with the band at 1385 cm<sup>-1</sup> observed by Pereira da Silva et al.<sup>49</sup> in the 632.8-nm excitation resonance Raman spectrum of secondary doped PANI–CSA/*m*-cresol sample. These last authors attributed the observation of this band using the 632.8-nm excitation radiation is an indication of the high concentration of free charge carriers in their secondary doped sample. On the basis of these considerations, we can evaluate that when the hybrids were obtained with the minor amount of polymer, the formed PANI has a conformation similar to that observed in secondary doped PANI.

Reflectance UV-vis spectra of hybrid samples are shown in Figure 3. The spectrum of pure (Ti,Sn)O<sub>2</sub> is also shown. Clearly, the hybrid samples present characteristic bands of polyaniline–emeraldine salt at ~320 nm, ~415 nm, and ~700–850 nm, which are attributed to  $\pi$ – $\pi^*$ , polaron– $\pi^*$ , and  $\pi$ –polaron transitions, respectively.<sup>51</sup> As can be seen in Figure 3, with increased content of polyaniline, the band attributed to the  $\pi$ –polaron transition is shifted from 844 nm (TiSn/PANI-1A and TiSn/PANI-2A, e and d, respectively, in Figure 3) to 700 nm (TiSn/PANI-1B and TiSn/PANI-2B, c and b, respectively, in Figure 3). Similar results were observed in hybrid samples obtained in a similar way, but using TiO<sub>2</sub> than (Ti,Sn)O<sub>2</sub> as the inorganic fraction.<sup>52</sup> These results would indicate that the polarons in the hybrids obtained with the minor amount of PANI are more delocalized than those in the other samples (as observed in secondary doped polyaniline)<sup>51,53</sup> and are in agreement with the appearance of the band at 1392 cm<sup>-1</sup> in the Raman spectra of these samples, as discussed before.

The X-ray diffraction patterns of pure (Ti,Sn)O<sub>2</sub> and TiSn/PANI hybrids are shown in Figure 4. The mixed oxide is formed mainly with the anatase structure (in

(45) Quillard, S.; Berrada, K.; Lovarn, G.; Lefrant, S.; Lapkowski, M.; Pron, A. *New J. Chem.* **1995**, *19*, 365.

(46) Furukawa, Y.; Hara, T.; Hyoto, Y.; Harada, I. *Synth. Met.* **1986**, *16*, 189.

(47) Sariciftici, N. S.; Bartonek, M.; Kuzmany, H. *Synth. Met.* **1989**, *29*, E193.

(48) Louarn, G.; Lapkowski, M.; Quillard, S.; Pron, A.; Buisson, J. P.; Lefrant, S. *J. Phys. Chem.* **1996**, *100*, 6998.

(49) Pereira da Silva, J. E.; Temperini, M. L. A.; Torresi, S. I. C. *Electrochim. Acta* **1999**, *44*, 1887.

(50) Engert, C.; Umapathy, S.; Kiefer, W.; Hamaguchi, H. *Chem. Phys. Lett.* **1994**, *218*, 87.

(51) Xia, Y.; Wiesinger, M.; MacDiarmid, A. G. *Chem. Mater.* **1995**, *7*, 443.

(52) Schnitzler, D. C.; Zarbin, A. J. G. to be published.

(53) Kuo, C.-T.; Chen, C.-H. *Synth. Met.* **1999**, *99*, 163.

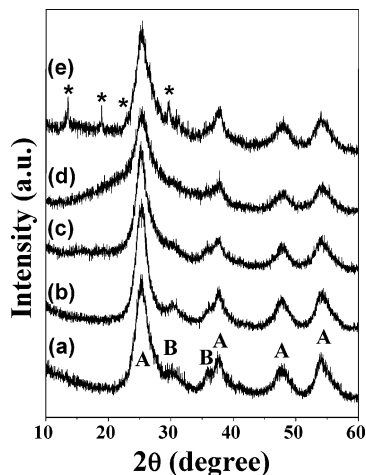


**Figure 4.** XRD pattern: (a)  $(\text{Ti,Sn})\text{O}_2$ ; (b)  $\text{TiSn/PANI-1A}$ ; (c)  $\text{TiSn/PANI-1B}$ ; (d)  $\text{TiSn/PANI-2A}$ ; (e)  $\text{TiSn/PANI-2B}$ . A = anatase, B = brookite.

which peaks are marked with A in the diffractogram present in Figure 4a) with traces of brookite (peaks marked with B in the Figure 4a). The XRD patterns of the hybrid samples present the same profile observed in the pure mixed oxide, indicating that the structure of the oxide was not modified by the polyaniline. Also, these results indicate that the polyaniline is amorphous in the hybrids. However, the XRD profile of the sample  $\text{TiSn/PANI-2B}$  (Figure 4e) presents, beyond the oxide peaks, four new peaks (marked with asterisks in Figure 4e) at  $13.44$ ,  $19.01$ ,  $23.14$ , and  $29.71^\circ$  (in  $2\theta$ ), indicating the formation of a new phase. According to the TG data

discussed earlier, the  $\text{TiSn/PANI-2B}$  sample shows the highest amount of polyaniline among all four hybrids discussed here, and despite the fact that this new phase is not well-known, it is clear that the results show improvement in the PANI amount. Gurunathan et al.<sup>32</sup> and Feng et al.<sup>30</sup> also observed new peaks in the XRD pattern of hybrids formed between colloidal  $\text{TiO}_2$  and polyaniline and these are attributed to a cross-linking of the polyaniline<sup>32</sup> or to a more ordered arrangement of the polymer in the composite samples, when compared with pure polyaniline.<sup>30</sup>

The broad peaks observed in all hybrids XRD pattern indicate short crystallite diameter of the oxide, which was estimated by the Scherrer's equation as 3.2 nm. Results obtained by Scherrer's equation suggest that the  $(\text{Ti,Sn})\text{O}_2$  crystallite size is not affected by the polymer presence and is approximately the same in the pure oxide and in all the hybrids materials.

Figure 5 shows the TEM photograph of the hybrid samples obtained according to the experimental procedure described for group 1, and Figure 6 shows the TEM images of the samples from group 2. As observed by the other characterization techniques, there is little difference between the TEM data obtained for the two samples that contain minor polymer amount, as well as between the two samples that contain the higher polymer amount. The TEM photograph of sample  $\text{TiSn/PANI-1A}$  (Figure 5a,b) and of the sample  $\text{TiSn/PANI-2A}$  (Figure 6a,b) show that the polymerization occurs on the surface of the spherical oxide particles, resulting in a well-defined core-shell  $(\text{Ti,Sn})\text{O}_2/\text{polyaniline}$  nano-

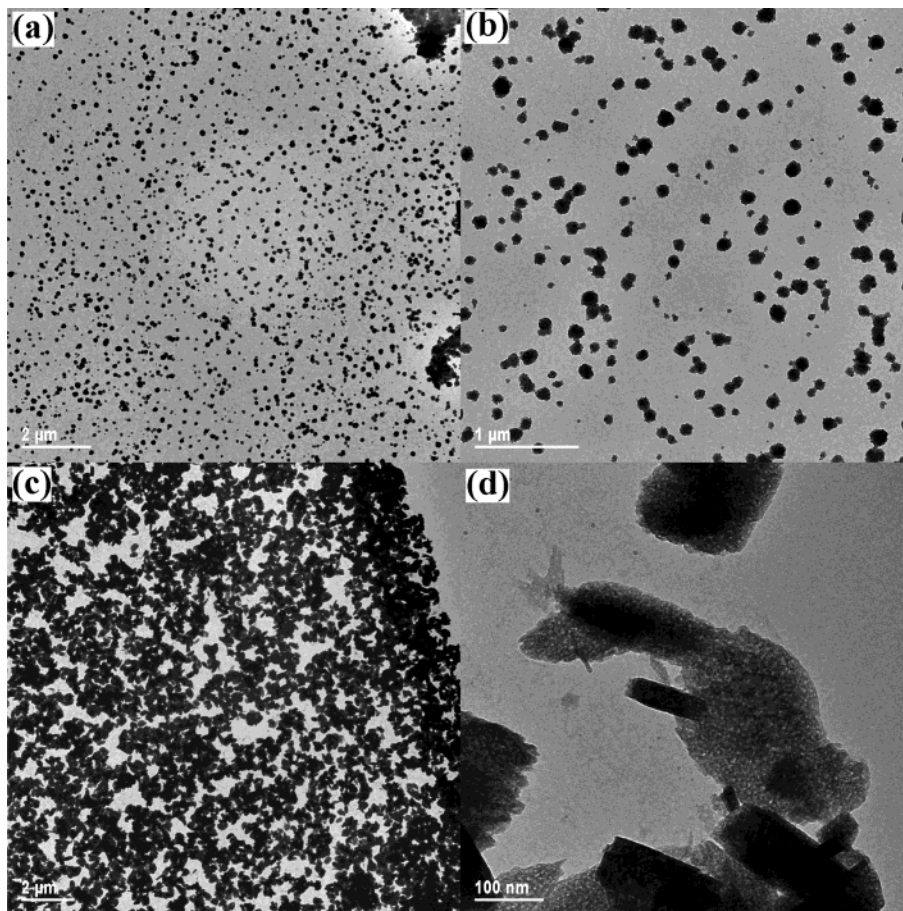


**Figure 5.** TEM photograph of the samples  $\text{TiSn/PANI-1A}$  (a and b) and  $\text{TiSn/PANI-1B}$  (c and d).

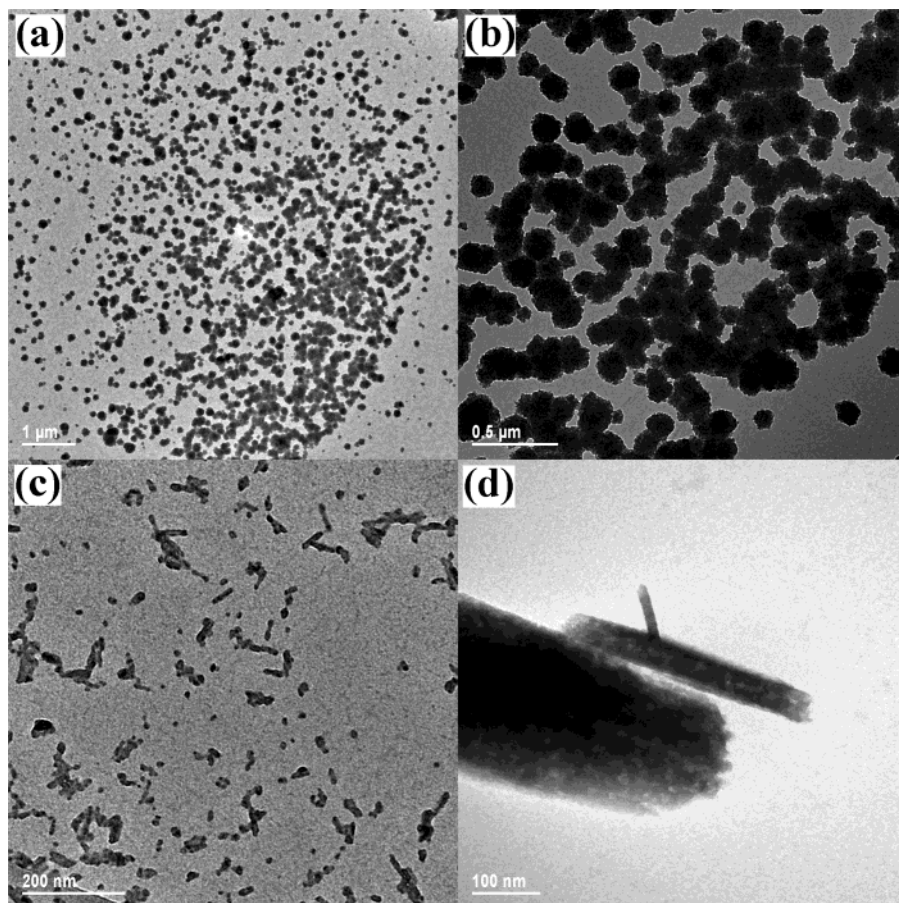


**Figure 6.** TEM photograph of the samples TiSn/PANI-2A (a and b) and TiSn/PANI-2B (c and d).

composite, similar to the  $\text{TiO}_2$ /polyaniline obtained under ultrasonic irradiation by Xia and Wang.<sup>33</sup> On the other side, the TEM photograph of sample TiSn/PANI-1B (Figure 5c,d) and of sample TiSn/PANI-2B (Figure 6c,d), show the oxide nanoparticles imbedded in a polymer mass. The occurrence of a core-shell nanocomposite in the lower amount polymer hybrids and the non-occurrence in the higher amount polymer will be discussed later. An interesting effect observed in Figures 5 and 6 is that the oxide presents tubular morphology in the higher polymer hybrids. The occurrence of this tubular morphology could be related to the excess of aniline present on the reactional media, resulting in morphology changes in the former oxide, in a similar way as reported by the utilization of bases such as tetramethylammonium hydroxide, aiming to control both size and shape of titanium oxide nanoparticles.<sup>54</sup> It is interesting to note that the tubular morphology occurs in both the high aniline content synthesis from group 1 or group 2 when the oxide nanoparticles were already formed previously to the addition of aniline. We do not yet have explanation for this and further studies will be necessary to understand this fact.

In the samples where the occurrence of core-shell was observed, we can suppose that the polymer chain shows organization around the oxide surface, which can promote expansion of the chains and high interchain interactions. In this case the molecular conformation will be more related to an "expanded coil" characteristic of secondary doped polyaniline,<sup>51,55</sup> and this conformation should explain the observation of the Raman and UV-vis signal of secondary doped polyaniline discussed

earlier. In the other samples, the oxide is imbedded in a polymer mass in which the main region is formed with the polymer chain conformed as a compact coil structure, typical of a non-secondary doped polyaniline. This explains the blue shift observed in the  $\pi$ -polaron band in the electronic spectrum of these samples.

Cyclic voltametry experiments were done and the results are shown in Figure 7. The voltammograms of all hybrids show two well-defined reversible redox process characteristic of polyaniline, confirming that the polymer shows electroactivity in the hybrids. During the voltammogram acquisition, the typical polyaniline color changes are observed, showing that the materials present electrochromism.

Figure 8 shows conductivity vs current density plots of the samples and the effect of the polyaniline content on it. As we can see, the conductivity values are dependent on the amount of polyaniline present in each sample. For example, it is observed that the conductivity of both lower polyaniline content samples is very near (as well as the polyaniline percent) and does not depend on the route employed to the sample synthesis. The film conductivity increases 1 order of magnitude to TiSn/PANI-1B sample (intermediate amount of polyaniline) and increases 2 orders of magnitude to TiSn/PANI-2B (maximum amount of polyaniline). Additionally, it is important to mention that the conductivity of the higher PANI content samples remains stable up to the highest measured current densities.

In the case of the TiSn/PANI-1A sample, we observed an increase of conductivity with increasing current

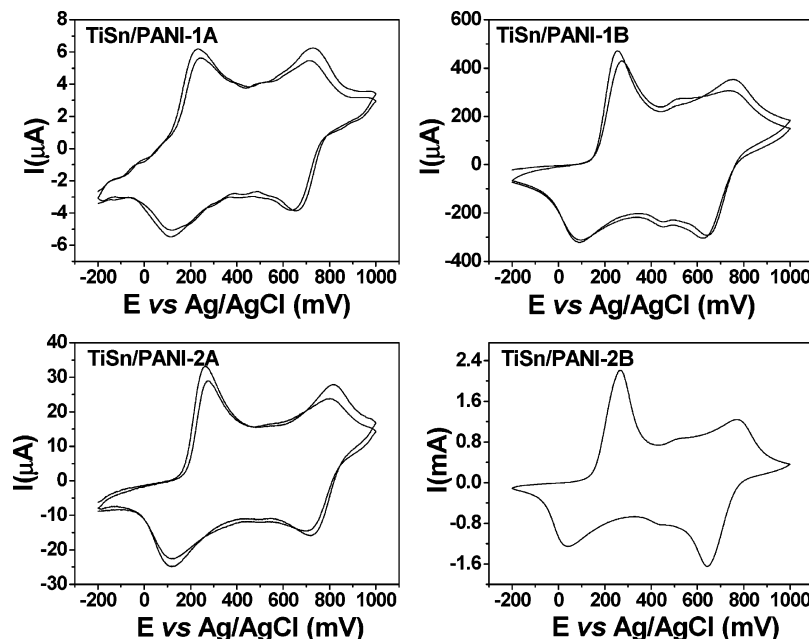


Figure 7. Cyclic voltammograms of the hybrid samples.

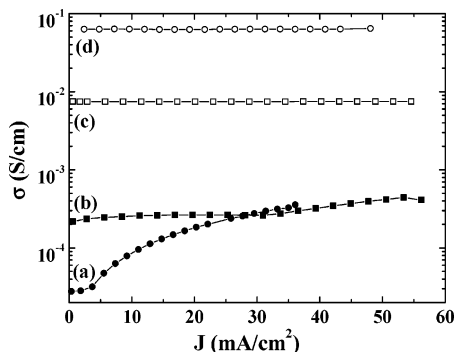


Figure 8. Conductivity of TiSn/PANI hybrid films as a function of current density: (a) TiSn/PANI-1A; (b) TiSn/PANI-2A; (c) TiSn/PANI-1B; (d) TiSn/PANI-2B.

density up to the highest measured current density value, at which these samples stopped conducting, appearing cracked. For this reason, it was not possible to test the reversibility of the conductivity, when the current density is decreased, back to its initial value. Furthermore most films of these samples cracked just after preparation. We succeeded in measuring the conductivity in only one film so this measurement may not be representative, deserving further investigation.

Another important conclusion obtained from the conductivity measurements is that the conductivity improvement with the polyaniline amount is not linear, which can indicate that the structure of the polyaniline formed in each sample and the kind of interaction between the polymer and the mixed oxide has an important role in the hybrid conductivity. Deeper studies into these effects will be done.

The results obtained by the different characterization techniques presented here can indicate that except by the resulting amount of polymer, the synthetic route employed to the hybrids (group 1 or group 2) does not show a strong influence on the characteristics of the

final product. The presence of aniline in the reactional media during the hydrolysis of the titanium isopropoxide plus tin chloride mixture apparently does not affect the structure of the former oxide, but a high amount of aniline changes its morphology. The fact that the amount of PANI obtained in the TiSn/PANI-2B is higher than that obtained in the TiSn/PANI-2A (despite the amount of initial monomer being the same) can indicate that when the oxide was formed in the media which already contains the monomer (group 1), part of this monomer was retained in the porous structure of the oxide and was not polymerized by the ammonium persulfate. As this unpolymerized aniline was not detected in the final hybrids, it should be eliminated during the successive washing steps.

Our model to the hybrid formation is the following: the aniline monomer gets adsorbed on the oxide particles (which were well-dispersed in the reactional media) and polymerization proceeds on the surface of the oxide particles when the persulfate solution was added. The adsorption of the aniline molecules on the oxide surface was confirmed when the oxide was isolated before the addition of the persulfate solution.<sup>52</sup> In the samples in which the initial amount of aniline was lower, we can suppose that all the added aniline was initially adsorbed on the oxide surface (once there are more surfaces available than aniline molecules to be adsorbed) and all aniline was polymerized as a shell of oxide nanoparticles. On the other hand, when the initial amount of aniline was higher, the polymerization began on the oxide surface and involved the excess of nonadsorbed aniline molecules, and the resulting material was formed by oxide nanoparticles encrusted in a free-polymer mass. The results obtained by TEM corroborate this hypothesis.

## Conclusions

Novel nanocomposites formed from  $(\text{Ti},\text{Sn})\text{O}_2$  and the conducting form of polyaniline were successfully obtained. The results showed here indicate that the main

(54) Chemseddine, A.; Moritz, T. *Eur. J. Inorg. Chem.* **1999**, 235.

(55) MacDiarmid, A. G.; Epstein, A. J. *Synth. Met.* **1995**, 69, 85.

characteristics of the nanocomposites are not affected by the two different preparation routes presented (which was based on the moment of aniline addition in the reactional media), but are strongly affected by the amount of monomer added prior to polymerization. This observation indicates that regardless of the aniline being present during the oxide formation or being added after it, its adsorption on the oxide surface before the polymerization apparently is the dominant step of the process. With control of the amount of aniline added to reaction, it was possible to produce a novel oxide-polymer core-shell material, or higher polymer content

hybrids with tubular morphology to a mixed oxide. Studies on photocurrents of these samples will be done as soon as possible.

**Acknowledgment.** This work was supported by CNPq and Rede de Materiais Nanoestruturados (MCT). Authors thank Laboratório de Espectroscopia Molecular (LEM-IQ-USP) by the Raman spectra, Centro de Microscopia Eletrônica-UFPR and Mrs. Marcela M. Oliveira by the TEM measurements.

CM034292P